Multiple Time-Scale Behavior of the Hydrogen-Bond Network in Water†

Anirban Mudi and Charusita Chakravarty*

Department of Chemistry, Indian Institute of Technology-Delhi, Hauz Khas, New Delhi 110016, India

Received: May 12, 2004; In Final Form: August 13, 2004

The temperature-dependent changes in the hydrogen-bond network of SPC/E water have been examined using power spectral analysis of fluctuations in tagged-molecule potential energies and local tetrahedral order parameters. The clear signatures of multiple time-scale or $1/f^{\alpha}$ behavior in the power spectra are shown to depend sensitively on the strength of hydrogen bonding. The analysis focuses on three specific power spectral features: the frequency of crossover to white noise behavior, the exponent in the $1/f^{\alpha}$ regime, and the librational peak. The exponent of the tagged-particle potential-energy fluctuations is shown to be strongly correlated with the diffusivity in the temperature range of 230 to 300 K. This correlation is strongest in the temperature−density regimes where the mechanism for diffusion is likely to be dominated by translational−rotational coupling, suggesting that the value of the exponent is a measure of the efficiency of the coupling of librational modes with network vibrations. The temperature dependence of all power spectral features was found to be strongest along the 0.9-g cm^{-3} isochore, which corresponds closely to the density of minimum diffusivity for the temperature range studied here. The static distributions of the tagged-particle quantities were examined to determine the degree of heterogeneity of the local molecular environment and its relationship with power spectral features.

1. Introduction

Water displays a number of thermodynamic and kinetic anomalies when compared to simple molecular and atomic liquids.[1,2,3,4] The density anomaly corresponds to a region of the phase diagram for which the density increases with temperature; this anomalous regime terminates at a temperature of maximum density (TMD). Because the TMD for water at standard pressure occurs at 4 °C, it is probably the most familiar of the anomalous properties of water. Many other anomalies become apparent only on supercooling water, such as the diffusional anomaly, which corresponds to an increase in molecular mobility with pressure; for example, translational diffusion in water at 243 K increases by 60% upon going from a pressure of 0.1 to 150 MPa.[5] Other measures of molecular mobility, such as inverse viscosity and inverse reorientational correlation times, also show a similar increase with density or pressure in the region of the diffusional anomaly. In addition to the anomalous density dependence, a number of transport properties of water also show an unusual temperature dependence, frequently fitted by a power law of the form $X = A_X(T/T_s - 1)^{\gamma}$, where X is some transport property such as the diffusivity. This behavior suggests that there exists a unique temperature of structural arrest, T_s, located at approximately 227 K in the case of water.

The unusual properties of water, in comparison to simple liquids, must be due to differences in the underlying potential-energy surface. Interactions in simple liquids are dominated by steep, short-range repulsions and long-range, isotropic attractions; consequently, the structure of simple liquids is dominated by short-range order and can be related to random close-packing arrangements of hard spheres. In contrast, the structure of water is dominated by strongly anisotropic hydrogen-bonding interactions. Because each water molecule can form at most four hydrogen bonds, a local tetrahedral geometry around each oxygen atom is strongly favored and results in an open, tetrahedral-network structure. The strength of the hydrogen bonds is estimated to lie between 5 and $10k_BT$ at melting.[6] Although this is strong enough that a substantial fraction of hydrogen bonds will be intact at room temperature, the thermal fluctuations will be large enough to ensure that such bonds will have a finite lifetime on the order of picoseconds; as a result, the dynamics of the liquid, especially in the supercooled states, will be dominated by the behavior of the three-dimensional hydrogen-bonded network, parts of which are constantly broken and reformed. Our focus in this work is to understand the relationship between these two crucial structural features of water, the local tetrahedral geometry and a fluctuating network of intermolecular hydrogen bonds, and the temperature dependence of the diffusivity.

We used molecular dynamics simulations of the extended simple point charge (SPC/E) intermolecular potential model for water. This model has been extensively studied and is known to reproduce many of the thermodynamic and kinetic anomalies of water. The calculations of the equation of state of SPC/E water predict that the TMD should lie at 242 K, which is approximately 35 K below the experimental value.[7,8,9] An analysis of the transport properties indicates a kinetic transition at 193 K along the 1-g cm^{-3} isochore, again shifted by about 35 K relative to the experimental value of 227 K.[8] As a function of density, the anomalous diffusional regime has been identified in the temperature range of 210 to 260 K.[10,11,12] Along a given isotherm, this region is demarcated by densities ρ_{min} and ρ_{max} corresponding to the minimum and maximum in the diffusivity. At 230 K, ρ_{min} is close to the ice density of 0.915 g cm^{-3} and

† Part of the special issue "Frank H. Stillinger Festschrift".

* Corresponding author. E-mail: charus@chemistry.iitd.ernet.in. Tel: +(91) 11 26591510. Fax: +(91) 11 2686 2122.

10.1021/jp047974o CCC: $27.50
Published on Web 10/01/2004

ρ_{max} is approximately 1.1 g cm^{-3}; ρ_{min} shows a smaller temperature dependence than ρ_{max}. Stretching water to densities below 0.85 g cm^{-3} creates inhomogeneous, phase-separated or cavitated structures. The SPC/E model is now frequently used to test theoretical ideas regarding the unusual static and dynamic properties of water, such as measures for spatiotemporal heterogeneity and possible connections between the different anomalies.[13,14,15]

The unusual dynamical properties of water must be related to the presence of the hydrogen-bond network; however, establishing a quantitative connection between the complex dynamics of a fluctuating network and a long-time averaged transport property, such as the diffusivity, is not trivial. Networks are typically characterized by multiple time scales because of the coupling of a large number of sites. In the case of water, the rotational and translational modes of individual molecules are strongly modified by the tetrahedral network and are better described as librations and intermolecular vibrations. The intermolecular vibrational frequencies can be thought of as cooperative rearrangements on different size and time scales that increase with the number of molecules involved; thus, the hydrogen-bonded network will have a multiplicity of time scales, starting with librational modes, two-molecule O−O stretches, three-molecule O−O−O bends, and so forth. Thermal fluctuations or steric crowding will tend to attenuate the network connectivity and multiple time-scale behavior. Multiple time-scale behavior is known to give rise to a stretched exponential behavior in the time-correlation functions, $C(t)$, with $C(t) = C(0)\exp[-(t/\tau)^{\beta}]$ and a $1/f^{\alpha}$-type dependence on the frequency f in the corresponding power spectrum, $S(f)$.[16] The extent and the frequency range over which a particular quantity will show multiple time-scale behavior will vary depending on the degree of sensitivity of the corresponding mechanical variable to motions on different time scales.

A number of different experimental techniques have been used to explore $1/f^{\alpha}$ behavior of bulk liquid water or the equivalent stretched exponential behavior of the time-correlation functions. The background intensity of the Raman spectrum of liquid water in the frequency range of 20−4500 cm^{-1} was fitted to a $1/f^{\alpha}$ form with $\alpha \approx 1.3$.[17] Dielectric relaxation measurements, however, yield single exponential or Debye-type relaxation behavior.[18] Inelastic neutron scattering experiments yield correlation functions that are consistent with the stretched exponential behavior.[19,20,21] Most recently, optical Kerr effect measurements have shown that the temperature dependence of the stretched exponential behavior is consistent with the predictions of the mode-coupling theory.[22] Although many, but not all, of the experimental techniques show evidence for stretched exponential behavior, it is difficult to extract information on the underlying microscopic origins of multiple time-scale behavior from experiment.

MD simulations allow for the monitoring of dynamical quantities that are inaccessible experimentally. This can be used to understand the microscopic origin of the $1/f^{\alpha}$ behavior in liquid water. An initial study of a TIPS2 model of water showed that fluctuations in the total inherent structure and tagged-particle potential energies gave rise to a $1/f^{\alpha}$ regime in the power spectrum.[23] We have recently shown that many of the tagged-particle quantities related to the local molecular environment show pronounced $1/f^{\alpha}$ behavior in the corresponding power spectra.[24,25,26] Moreover, the frequency range of $1/f^{\alpha}$ behavior and the value of the exponent α carry significant dynamical information; for example, the variations in mobility with density in the region of the diffusional anomaly are unambiguously mirrored in the exponent of the $1/f^{\alpha}$ region, and the frequency range of multiple time-scale behavior provides a quantitative measure of the time and length scales over which correlations in the network die out.

In this work, the $1/f^{\alpha}$ behavior in the power spectra is related to the underlying static distributions for the local order as well as the tagged-molecule configurational energies. We show how variations in the temperature or in the potential-energy surface result in correlated changes in the static and dynamic behavior of the tagged-particle quantities. The paper is organized as follows. Section 2 states the essential results of power spectral analysis used in this work and defines the tagged-particle quantities of interest from the point of view of understanding hydrogen-bond network dynamics. Section 3 gives the details of the molecular dynamics simulations. Section 4 contains a discussion of our results, and Section 5 summarizes the conclusions.

2. Power Spectral Analysis

2.1 Signatures of Multiple Time-Scale Behavior. Given any mechanical quantity $A(t)$ as a function of time t, one can define the power spectrum of the fluctuations about the mean, $\langle A\rangle$, as

$$S(f) = \left|\int_{t_{min}}^{t_{max}} (A(t) - \langle A\rangle) e^{2\pi i f t}\, dt\right|^2 \tag{1}$$

Consider a situation in which there is a single relaxation frequency λ in the system. If several such relaxation events take place at an average rate n at times t_k, $k = 1, 2,...$, then each event will give rise to an exponential decay in some appropriate dynamical variable of the form $A(t, t_k) = A_0 \exp[-\lambda(t - t_k)]$ for $t \geq t_k$ and $A(t, t_k) = 0$ for $t \leq t_k$, giving rise to an overall time-dependent signal $A(t) = \sum_k A(t, t_k)$. The power spectrum corresponding to such a time signal will be of the form[27,28]

$$S(f) = \frac{A_0^2 n}{\lambda^2 + f^2} \tag{2}$$

corresponding to $1/f^2$ for Lorentzian behavior in the limit $f \gg \lambda$. If, however, the relaxation frequencies are uniformly distributed over the range of λ_1 to λ_2 and the amplitude of each pulse remains constant, then

$$S(f) = \frac{1}{\lambda_2 - \lambda_1}\int_{\lambda_1}^{\lambda_2} \frac{A_0^2 n}{\lambda^2 + f^2} d\lambda$$

$$= \frac{A_0^2 n}{f(\lambda_2 - \lambda_1)}\left[\arctan\left(\frac{\lambda_2}{f}\right) - \arctan\left(\frac{\lambda_1}{f}\right)\right] \tag{3}$$

In the low-frequency limit where $f \ll \lambda_1 \ll \lambda_2$, a white noise region with $S(f) = A_0^2 n$ will be seen. In the intermediate regime where $\lambda_1 \ll f \ll \lambda_2$, one will obtain

$$S(f) = \frac{A_0^2 n \pi}{2f(\lambda_2 - \lambda_1)} \tag{4}$$

which corresponds to the $1/f^{\alpha}$ regime with $\alpha = 1$. In the high-frequency limit for which $f \gg \lambda_2 \gg \lambda_1$, one will obtain a Lorentzian tail with $S(f) = A_0^2 n/f^2$. Other distributions of time scales may also give rise to $1/f^{\alpha}$ behavior; for example, a distribution $P(\lambda) \propto 1/\lambda^{1+\beta}$ over the same frequency interval will generate $S(f) \propto 1/f^{1+\beta}$. In general, an exponent lying between 0.5 and 1.5 may be taken to be an indication of multiple time-

scale dynamics, whereas exponents close to 2 indicate single time-scale behavior. We show that the range of $1/f^{\alpha}$ behavior and the associated exponent carry significant information about the dynamical behavior of water.

2.2 Observable Properties. In this study, we focus on dynamical correlations in observable properties that will be sensitive to the local molecular environment. Such properties will be intensive, rather than extensive and, therefore, will not be subject to decreasing signal-to-noise ratios with increasing system size. More interestingly, these are the properties that are likely to be most strongly affected by network formation due to hydrogen bonding. Power spectra of a number of such tagged-particle properties have been recently studied by us; for example, tagged-particle kinetic and potential energies, local order parameters, and coordination numbers.[24,25,26] In this work, we have focused particularly on the behavior of the power spectra associated with fluctuations in the tagged-molecule potential energies and local tetrahedral order because these have been shown to be the most sensitive to different time scales of the hydrogen-bond network.

Tagged-Molecule Potential Energy. The tagged-molecule potential energy, $u(t)$, corresponds to the interaction energy of an individual molecule with all of the other molecules in the system. Because the configurational potential energy is assumed to be pair additive, the total potential energy is $U(t) = 0.5\sum_i u_i(t)$, where the sum extends over all molecules. The key features of the corresponding power spectrum, denoted by $S_u(f)$, are (i) a broad peak due to the librational modes at approximately 500 cm^{-1}, which forms a shoulder at high temperatures or densities; (ii) a single $1/f^{\alpha}$ region at high temperatures spanning the 1−200 cm^{-1} range at 300 K, which separates into two $1/f^{\alpha}$ regions with different exponents at low temperatures; and (iii) a temperature-dependent crossover to white-noise behavior at low frequencies. The $S_u(f)$ spectra are, therefore, sensitive to the hydrogen-bond network reorganizations over a range of frequencies, including the librations and the O−O stretch and O−O−O bending modes that occur at 200 and 50 cm^{-1}, respectively, for SPC/E water.[29]

Local Tetrahedral Order. We used two different local order parameters, q_O and q_H, to characterize the degree of tetrahedrality of the four nearest-neighbor oxygen and hydrogen atoms, respectively. The q_H order parameter of a given oxygen atom i is measured by

$$q_H = 1 - \frac{3}{8}\sum_{j=1}^{3}\sum_{k=j+1}^{4}\left(\cos\psi_{jk} + \frac{1}{3}\right)^2 \qquad (5)$$

where ψ_{jk} is the angle between the bond vectors $\mathbf{r}_{ij}$ and $\mathbf{r}_{ik}$ and j and k label the four nearest hydrogen atoms. Because the four hydrogen atoms will never be equidistant from the central oxygen, q_H is purely an orientational order parameter. The q_O order parameter is similarly defined using the positions of the four nearest oxygen atoms. The q_O order parameter, in conjunction with a translational order parameter, has been used previously to characterize the region of the phase diagram within which anomalous diffusional and density dependence could be expected.[13,14]

The power spectra associated with fluctuations in the q_O and q_H values of tagged particles are denoted by $S_O(f)$ and $S_H(f)$, respectively. Both sets of power spectra show a multiple time-scale region crossing over to white noise at low frequencies. Whereas $S_H(f)$ shows a peak due to librational motion at low temperatures, $S_O(f)$ is insensitive to the relatively localized librational motion. At a given temperature and density, the crossover to white-noise behavior occurs at higher frequencies for $S_O(f)$ and $S_H(f)$ than for $S_u(f)$, indicating that the tetrahedral order decorrelates over a smaller spatial and temporal range than the potential energy.

3. Computational Details

3.1 The SPC/E Model. The SPC/E model for water assumes that the water molecule can be treated as a rigid, nonpolarizable entity.[30] Each water molecule carries three charged sites that are located at the atomic positions and are associated with the corresponding atomic masses. The OH distance is 1.0 Å, and HOH angle is equal to 109.47°, with partial charges on oxygen and hydrogen of −0.8476e and +0.4238e respectively. The Lennard-Jones site is located at the oxygen atom, and the corresponding parameters are $\sigma = 3.166$ Å and $\epsilon = 0.6517$ kJ/mol. The configurational potential energy of the system is calculated by assuming pairwise additive interactions between water molecules.

3.2 Molecular Dynamics. The molecular dynamics (MD) simulations were performed using the DL_POLY software package.[31] NVT ensemble simulations for 256 SPC/E water molecules contained in a cubic simulation cell were carried out using the SHAKE algorithm with a time step of 1 fs. Electrostatic interactions were evaluated using Ewald summation.[32] A Berendsen thermostat was used to maintain the desired temperature. An appropriate value for the thermostat time constant(τ_B) was made after studying its effect on various dynamical quantities.[25] Within the statistical error bars, our simulation results match those reported in refs 7 and 8. There is a difference of approximately 1% between the ensemble-averaged potential energy reported in this work and that in ref 8, which may be attributed to the use of the Ewald summation, rather than a reaction field method, to account for long-range interactions.

Simulations were carried out at six temperatures (230, 250, 260, 280, 300, and 340 K) along seven isochores (0.75, 0.9, 1.0, 1.1, 1.2, 1.3, and 1.4 g cm^{-3}). At each state point, the system was equilibriated for a time period of 2 to 5 ns. Production run lengths were kept at 2 ns with $\tau_B = 200$ps. Additional runs were carried out at three temperatures (280, 300, and 340 K) with production run lengths of 8.4 ns and $\tau_B = 1000$ ps as a check of the results. Given the relatively large values of τ_B, our final temperatures were typically within 2 K of the desired temperature, but at low temperatures, deviations of up to 3 K were seen.

3.3 Generating Power Spectra. Tagged-particle quantities for 64 molecules were stored at intervals of 10 fs from the 2-ns production runs. This sampling interval corresponds to a Nyquist frequency of 1666 cm^{-1}. The values of τ_B provide the lower limit on the frequency range over which we can obtain reliable power spectra; thus,$\tau_B = 200$ ps corresponds to a lower frequency limit of 0.165 cm^{-1}. Standard fast Fourier transform routines were used with a square sampling window.[33] The normalization convention was chosen such that the integrated area under the $S(f)$ curve was equal to the mean square amplitude of the time signal. Windows containing 2^{15} data points were used for the Fourier transformation. Statistical noise in the power spectra was reduced by averaging over overlapping time-signal windows as well as over individual tagged-particle spectra. In a given frequency interval showing $1/f^{\alpha}$ behavior, linear least-squares fitting of ln $S(f)$ was done to obtain the α values. The variations in the α values that were calculated from three independent simulations for the densities 0.9, 1.1, and 1.4 g cm^{-3} at 230 K were found to be less than 2%.

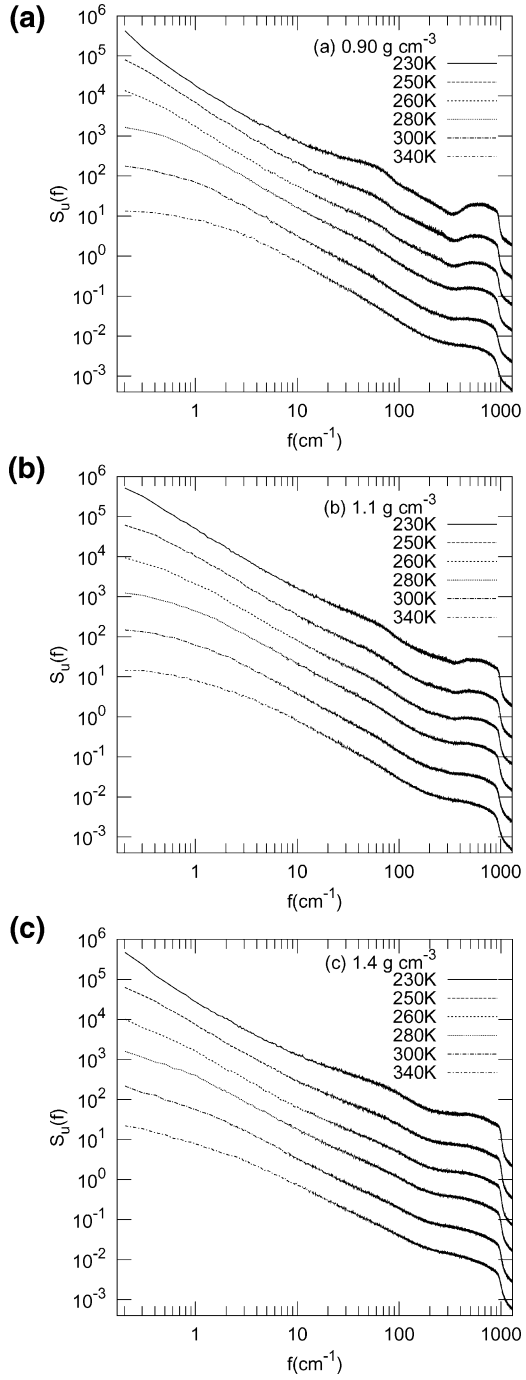

Figure 1. Spectrum of fluctuations of tagged particle potential energies at different temperatures for isochores corresponding to (a) 0.9, (b) 1.1, and (c) 1.4 g cm^{-3}.

4. Results and Discussion

4.1 Fluctuations in Tagged-Particle Potential Energies. *4.1.1. Power Spectra.* The temperature dependence of the power spectra associated with tagged-particle potential energies is first considered because this quantity has been found to be the most sensitive to the multiple time scales present in the hydrogen-bond network. Figure 1a shows $S_u(f)$ curves for different temperatures along the 0.9-g cm^{-3} isochore, which is close to ρ_{min}, the density corresponding to the diffusivity minimum. At 230 K, the librational peak is well defined, although the librational band is broad and stretches from 400 to 1000 cm^{-1}. There are two frequency domains showing $1/f^{\alpha}$ behavior: a low-frequency region up to 40 cm^{-1} with $\alpha_u \approx 1$ and a high-frequency region spanning 60−300 cm^{-1} with $\alpha_u' = 1.6 \pm 0.03$. The high-frequency region must include the O−O stretch (200 cm^{-1}) and the O−O−O bend (50 cm^{-1}). The discontinuity in slope at about 50 cm^{-1} suggests that the two-molecule, and possibly three-molecule, vibrational mode is partially decoupled from the other network vibrations. Given that α_u' is significantly higher than α_u, one can also think of this region as falling in the Lorentzian tail of the true $1/f$ regime lying below 40 cm^{-1}. As the temperature increases, the librational peak shifts to lower frequencies and eventually forms a shoulder in the $S_u(f)$ curve. Increasing thermal fluctuations also merge the two $1/f^{\alpha}$ regions to form a single multiple time-scale regime between 1 and 200 cm^{-1} for temperatures of 280 K and above. The crossover to white-noise behavior shifts to higher frequencies with temperature; at 280 K, it occurs at about 0.5 cm^{-1}. We note that even at 340 K, which would be close to the vaporization temperature for SPC/E water, there is still evidence of multiple time-scale behavior.

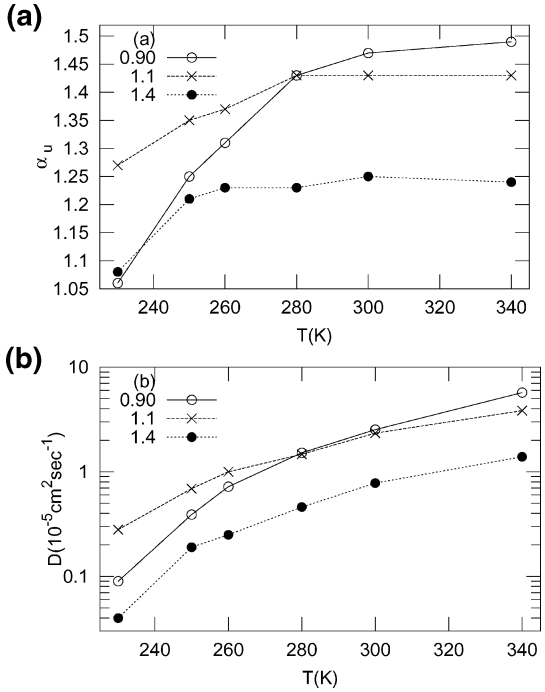

Figure 2. Temperature dependence of (a) exponent of the $1/f^{\alpha}$ region of the $S_u(f)$ curve and (b) diffusivity along the 0.9, 1.1, and 1.4 g cm^{-3}. The low-frequency multiple time-scale region between 1 and 40 cm^{-1} is used for evaluating α_u at temperatures below 280 K. At 280 and 300K, α_u is evaluated over the region of 1−200 cm^{-1}, whereas at 340 K, the $1/f^{\alpha}$region is taken from 3 to 200 cm^{-1}.

Our simulations show that the changes in the $S_u(f)$ curves with temperature are the most marked at densities close to ρ_{min}, corresponding to the diffusivity minimum. At higher densities (Figure 1b and 1c), the changes are less pronounced, although qualitatively similar to those seen at ρ_{min}. The frequency range of $1/f^{\alpha}$ behavior does not change substantially with density along a given isotherm, suggesting that this feature is determined largely by the magnitude of the thermal fluctuations relative to k_BT; for example, the O−O vibrational frequency corresponds to k_BT at 300 K. It is, therefore, not surprising that as the temperature decreases below this value a break develops in the slope of the ln $S_u(f)$ curve.

4.1.2. Connection between Diffusivity and the $1/f^{\alpha}$ Exponent. To quantify the effect of temperature on the multiple time-scale behavior, Figure 2a shows $\alpha_u(T)$ along three isochores. Above 300 K, essentially all of the network vibrations are strongly coupled with the librations and $\alpha_u(T)$ reaches a plateau at

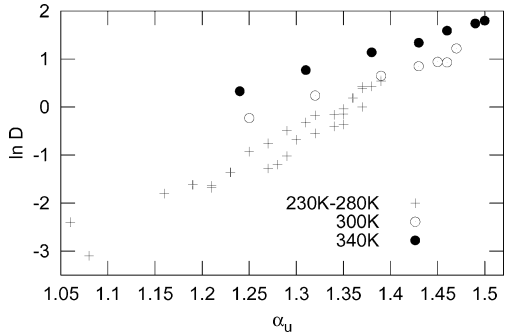

Figure 3. Correlation between ln D and α_u, the exponent of the $1/f^{\alpha}$ region of the $S_u(f)$ curve. D is in units of 10^{-5} cm^2 s^{-1}.

about 1.5. Below 300 K, the two-molecule vibrational mode gets progressively decoupled from the higher-order network rearrangements also resulting in a decoupling of librational modes. In our previous work on the correlation between the $1/f^{\alpha}$ exponents and the diffusional anomaly, it was suggested that coupling (decoupling) of high-frequency, localized librational modes should lead to an increase (decrease) in α_u.[26] It is, therefore, not suprising that a decrease in temperature results in a decrease in α_u.

Figure 2b shows the temperature dependence of the diffusivity. The parallels with the temperature dependence of α_u are apparent; for example, both quantities show the strongest temperature dependence along the 0.9-g cm^{-3} isotherm.The strong correlation between α_u and ln D is well illustrated by Figure 3. The correlation coefficient between α_u and ln D is 0.93 if the data from all of the simulated state points is used. If the data at 340 K are omitted, then $r = 0.96$; however, it does not significantly increase if the data at 300 K are also omitted. This can be explained by the assumption that α_u provides a suitable measure of the efficiency of coupling of librations to network vibrations. At temperatures between 230 and 300 K, the coupling of librations to network vibrations plays a crucial role in the molecular mechanism for diffusion and a strong correspondence between α_u and D is observed. For high temperatures or high densities lying outside the region of the diffusional anomaly, random thermal collisions will play the key role in determining diffusivity, as in the case of simple liquids, and the correlation between α_u and D will tend to break down.

It is interesting to consider what might happen to the correspondence between α_u and D as T approaches the mode-coupling transition temperature, T_{MC}. Simulations of SPC/E water indicate that D will approach zero as $T \rightarrow T_{MC}$. We can conjecture that multiple time-scale behavior will survive because the kinetic glass transition must be accompanied by an increase in spatiotemporal heterogeneity, although it will be shifted to lower frequencies. Upon reducing the temperature from 230 K to T_{MC} (190 K at 1 g cm^{-3}), the librational modes and the O−O stretches will be further decoupled from the higher-order network reaarangements. The strong correlation between α_u and D will only be observed if the frequency range of $1/f^{\alpha}$ behavior includes high-frequency, short-range rearrangement time scales of the hydrogen-bond network, implying that translational−rotational coupling continues to play an important role in determining diffusivity. The proof that this may be the case is suggested by the fact that the T_{MC} values for SPC/E vary with density and reach a minimum of 189 K close to ρ_{max} and increase to about 210 K at 1.4 g cm^{-3}. We note that our present results correlate trends in α_u and D. It would be of interest to explore further the nature of the dependence between the two quantities, especially close to the mode coupling temperature.

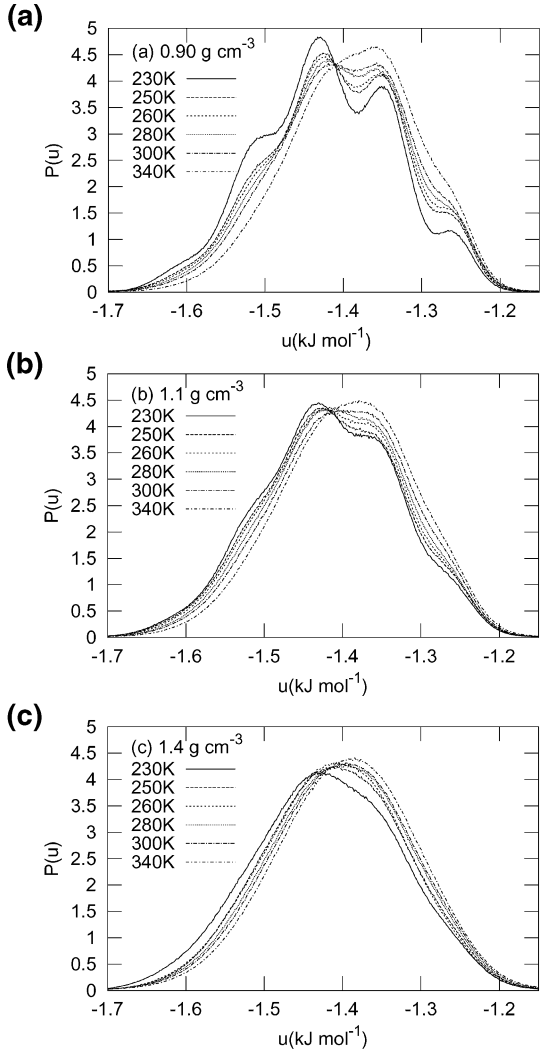

Figure 4. Static distribution of tagged particle potential energies (in kJ mol^{-1}) at different temperatures for isochores corresponding to (a) 0.9, (b) 1.1, and (c) 1.4 g cm^{-3}.

4.1.3. Static Distributions. We expect that the multiple time-scale behavior due to dynamical correlations in the tagged-particle configurational energies must reflect the diversity of the local molecular environments. To illustrate this connection between the static and dynamic properties of the hydrogen-bonded network, we calculated the equilibrium probability distributions of the tagged-particle potential energies (Figure 4). The most striking feature of the $P(u)$ distributions that can be correlated with the behavior of the power spectrum is the degree of multimodality. Multimodality is most pronounced along the 0.9-g cm^{-3} isochore along which local tetrahedral order is also known to be maximum. Increasing tetrahedral order promotes decoupling of librations from network vibrations, which can be seen as a discontinuity in the slope of ln $S_u(f)$ curves. The width of the distributions does not significantly change with the temperature or density, but the multimodality is clearly reduced by thermal fluctuations. Multimodality is also removed at higher densities; for example, at 1.4 g cm^{-3}, which lies in the normal diffusional regime, there is no evidence of multimodality.

4.2. Fluctuations in Local Tetrahedral Order. Figure 5 shows the $S_H(f)$ and $S_O(f)$ spectra at different densities along the 0.9-g cm^{-3} isochore. Other than the absence of the librational peak in $S_O(f)$, the temperature-dependent trends in the spectra above 20 cm^{-1} are very similar to those observed for $S_u(f)$;

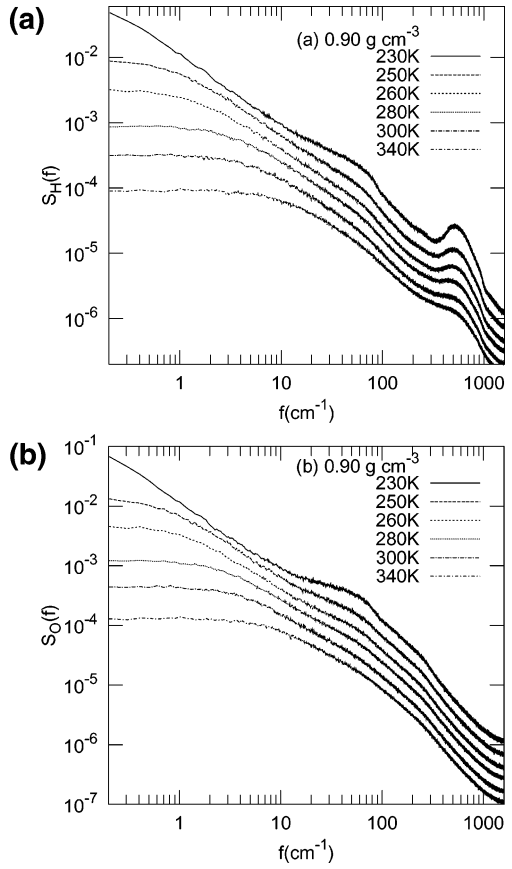

Figure 5. Power spectra due to fluctuations in tetrahedral order parameters. (a) $S_H(f)$ and (b) $S_O(f)$ curves at different temperatures along the 0.9-g cm^{-3} isochore.

however, the power spectra of fluctuations in these tetrahedral order parameters shows a crossover to white-noise behavior at much higher frequencies than the power spectra generated from tagged-particle potential energies. The increase in this crossover frequency with temperature is also noticeable. This suggests that tetrahedral order rapidly decorrelates over the hydrogen-bonded network and is very sensitive to temperature. Qualitatively, these conclusions are unsurprising, but we have not seen a similar quantitative measure of these effects previously.

Figure 6 shows the static distribution of the local order parameters. The bimodal character of the $P(q_O)$ distributions with increasing temperature has been previously pointed out. The $P(q_H)$ distributions have not been studied previously. They do not change significantly in terms of relative heights of peaks with temperature, suggesting that the hydrogen atom positions close to a given oxygen change little with temperature because of the strongly directional character and strength of the hydrogen bond. The width of the $P(q_O)$ and $P(q_H)$ distributions, unlike that of $P(u)$, varies significantly with temperature.

4.3 Modifying Power spectra by Varying the Strength of Hydrogen Bonding. The SPC/E model effectively condenses information about short-range repulsion and dispersion using Lennard-Jones terms. The long-range electrostatic interactions and anisotropic hydrogen-bonding interactions are controlled by the partial charge distribution. To study the effect of varying the strength of hydrogen bonding on the power spectra, we followed ref 34 and scaled the SPC/E charges. The effect on the power spectra as well as on the static distribution of tagged-particle potential energies at 230 K is shown in Figures 7 and 8, respectively. A slight increase in the SPC/E charges is sufficient to significantly decouple the O−O bending mode, in addition to the librations, from the multiple time-scale regime. The reduction of the charge on the oxygen atom from 0.8476e to 0.7e is sufficient to convert the librational peak into a shoulder and induce a crossover to white-noise behavior at frequencies below 5 cm^{-1}. The multimodal character of the corresponding

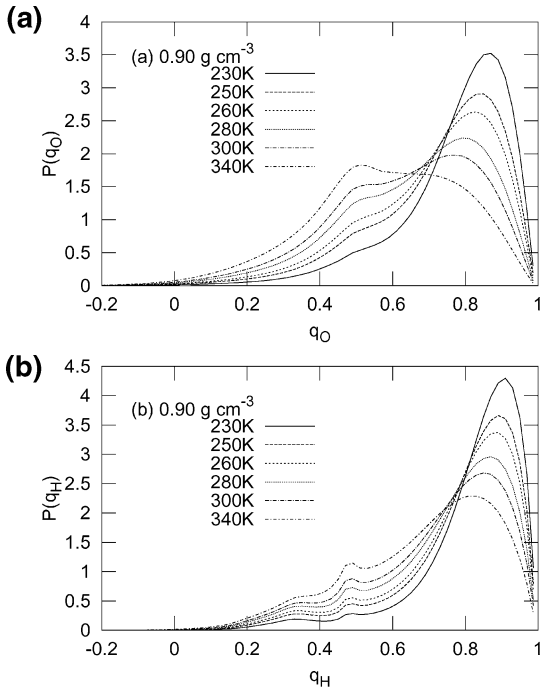

Figure 6. Static distribution of tetrahedral order parameters at different temperatures for isochores at 0.9 g cm^{-3} (a) $P(q_O)$ and (b) $P(q_H)$.

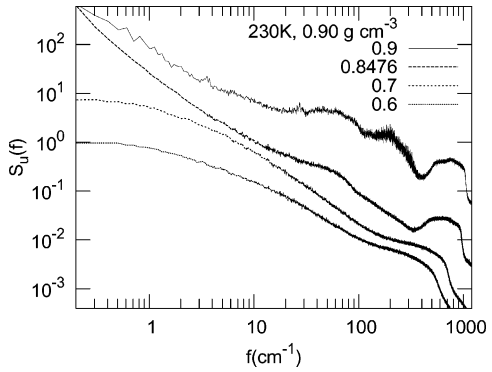

Figure 7. Spectrum of fluctuations of tagged particle potential energies, $S_u(f)$, for different scalings of SPC/E partial charge distributions at 230 K and 0.9 g cm^{-3}. The partial charge on the oxygen atom, in units of electronic charge, is shown in the graphical key.

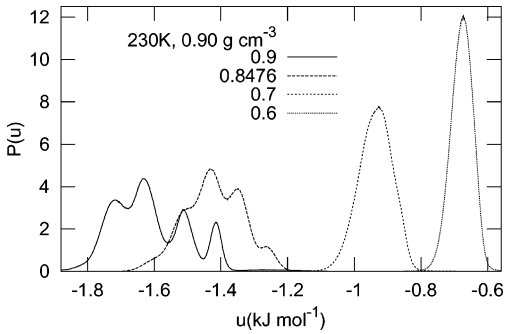

Figure 8. Static distributions of tagged particle potential energies (in kJ mol^{-1}) for different scalings of SPC/E partial charge distributions at 230 K and 0.9 g cm^{-3}. The partial charge on the oxygen atom, in units of electronic charge, is shown in the graphical key.

static distribution is also removed. Further reduction of the SPC/E charge leads to complete removal of any sign of multiple time-scale behavior. As the SPC/E charges are reduced and the system approaches a Lennard-Jones fluid in its behavior, the tagged-particle potential energy distributions narrow significantly, indicating that the heterogeneity in local molecular environments that is responsible for multiple time-scale behavior is lost.

5. Conclusions

The temperature-dependent changes in the hydrogen-bond network of SPC/E water have been examined using power spectral analysis of fluctuations in tagged-molecule configurational energies and local tetrahedral order. The signs of multiple time scale behavior in the power spectra are shown to depend sensitively on the strength of hydrogen bonding.

The analysis was focused on the following specific power spectral features: the frequency of crossover to white-noise behavior, the exponent of $1/f^{\alpha}$ behavior, and the librational peak. The librational peak loses its distinct identity as a function of increasing temperature, indicating that destruction of local tetrahedral order facilitates the coupling of librational modes to the network vibrations. The frequency of crossover to white noise also increases with temperature, indicating that correlated motions in the network have a shorter spatiotemporal range as the temperature increases. The crossover to white noise occurs at higher frequencies in the case of the tetrahedral order parameters. The diffusivity is shown to be strongly correlated with the exponent of the $1/f^{\alpha}$ region of the power spectra of the tagged-particle potential energy fluctuations, especially at temperatures of 300 K or below. We show that this exponent acts as a measure of the efficiency of the coupling of librational modes to the network vibrations; therefore, the strong correlation with diffusivity is observed in temperature−density regimes where the mechanism of diffusion is predominantly determined by translational−rotational coupling. For high temperatures or high densities lying outside the anomalous diffusional region, random thermal collisions will play a significant role in determining diffusivity and this correlation will be less strong. The temperature dependence of all power spectral features is strongest along the 0.9-g cm^{-3} isochore, which corresponds closely to the density of minimum diffusivity for the temperature range studied here. The static distributions of the tagged-particle configurational energies and tetrahedral order parameters were examined to establish the degree of heterogeneity of the local molecular environment, which could, in turn, be related to some of the power spectral features.

The key result of this work is the determination that power spectral analysis is a convenient and direct way of connecting different length and time-scale features of a networked liquid; for example, in the case of water, we can connect the local energy and order, the multiple time-scale behavior of the network, and an equlibrium transport property, the diffusivity. This type of analysis may be useful in exploring the connections between local order and the dynamical and static anomalies of water as well as in understanding aqueous solutions, networked liquids, and other hydrogen-bonded systems.

Acknowledgment. Financial support for this work has been provided by the Department of Science and Technology (SP/S1/H-16/2000). A.M. thanks the Council for Scientific and Industrial Research, New Delhi for the award of a Senior Research Fellowship. We thank R. Ramaswamy for discussions and R. Lynden-Bell for suggesting simulations with modified SPC/E water potentials.

References and Notes

(1) Stillinger, F. H. *Adv. Chem. Phys.* **1974**, *31*, 1.
(2) Debenedetti, P. G. *J. Phys.: Condens. Matter* **2003**, *15*, R1669.
(3) Franks, F.; Ed. *Water: A Comprehensive Treatise*; Plenum Press: New York, 1972.
(4) Angell, C. A. *Annu. Rev. Phys. Chem.* **1983**, *593*, 34.
(5) Prielmeier, F. X.; Lang, E. W.; Speedy, R. J.; Lüdeman, H. D. *Phys. Rev. Lett.* **1987**, *59*, 1128.
(6) Texeira, J. In *Hydration Processes in Biology*; Bellissent-Funel, M. C., Ed.; IOS Press: Amsterdam, 1999.
(7) Harrington, S.; Poole, P. H.; Sciortino, F.; Stanley, H. E. *J. Chem. Phys.* **1997**, *107*, 7443.
(8) Starr, F. W.; Sciortino, F.; Stanley, H. E. *Phys. Rev. E* **1999**, *60*, 6757.
(9) Arbuckle, B. W.; Clancy, P. *J. Chem. Phys.* **2002**, *116*, 5090. Note that the TMD for SPC/E water is found to be 260 K in this work; however, there are significant computational differences between this study and refs 7 and 8.
(10) Netz, P. A.; Starr, F. W.; Barbosa, M. C.; Stanley, H. E. *Physica A* **2002**, *315*, 470.
(11) Netz, P. A.; Starr, F. W.; Stanley, H. E.; Barbosa, M. C. *J. Chem. Phys.* **2001**, *115*, 344.
(12) Scala, A.; Starr, F. W.; Nave, E.; Sciortino, F.; Stanley, H. E. *Nature* **2000**, *406*, 166.
(13) Errington, J. R.; Debenedetti, P. G. *Nature* **318**, *2001*, 409.
(14) Errington, J. R.; Debenedetti, P. G.; Torquato, S. *Phys. Rev. Lett.* **2002**, *89*, 215503.
(15) Giovambattista, N.; Buldyrev, S. V.; Starr F. W.; Stanley, H. E. *Phys. Rev. Lett.* **2003**, *90*, 085506.
(16) Elliot, S. R. *Physics of Amorphous Materials*; Longman Scientific and Technical: Essex, U.K., 1990.
(17) Walrafen, G. E.; Hokmabadi, M. S.; Yang, W. H.; Chu, Y.-C.; Monosmith, B. *J. Phys. Chem.* **1989**, *93*, 2909.
(18) Bertollini, D.; Cassettrari, M.; Ferrario, M.; Grigolini, P.; Salvetti, G. *Adv. Chem. Phys.* **1985**, *62*, 277.
(19) Gallo, P.; Sciortino, F.; Tartaglia, P.; Chen, S.-H. *Phys. Rev. Lett.* **1996**, *76*, 2730.
(20) Chen, S.-H.; Liao, C.; Sciortino, F.; Gallo P.; Tartaglia, P. *Phys. Rev. E* **1999**, *59*, 6708.
(21) Bellisent-Funel, M.-C.; Longeville, S.; Zanotti, J. M.; Chen, S.-H. *Phys. Rev. Lett.* **2000**, *85*, 3644.
(22) Torre, R.; Bartolini, P.; Righini, R. *Nature* **2004**, *428*, 296.
(23) Sasai, M.; Ohmine, I.; Ramaswamy, R. *J. Chem. Phys.* **1992**, *96*, 3045.
(24) Mudi, A.; Ramaswamy, R.; Chakravarty, C. *Chem. Phys. Lett.* **2003**, *376*, 683.
(25) Mudi, A.; Chakravarty, C. *Mol. Phys.* **2004**, *102*, 683.
(26) Mudi, A.; Ramaswamy, R.; Chakravarty, C. (http://arXiv.org/abs/cond-mat/0405210).
(27) Milotti, E. *Phys. Rev. E* **1995**, *51*, 3087.
(28) Milotti, E. (http://arXiv.org/abs/physics/0204033).
(29) Parker, M. E.; Heyes, D. M. *J. Chem. Phys.* **1998**, *108*, 9039.
(30) Berendsen, H. J. C.; Grigera, J. R.; Straatsma, T. P. *J. Phys. Chem.* **1987**, *91*, 6269.
(31) Smith, W.; Yong C. W.; Rodger, P. M. *Mol. Simul.* **2002**, *28*, 385. The DL_POLY website is http://www.cse.clrc.ac.uk/msi/software/DL_POLY/.
(32) Allen, M. D.; Tildesley, D. J. *Computer Simulation of Liquids*; Clarendon Press: Oxford, U.K., 1986.
(33) Press: W. H.; Flannery, B. P.; Teukolskyi, S. A.; Vetterling, W. T. *Numerical Recipes in Fortran*; Cambridge University Press: Cambridge, U.K., 1990.
(34) Bergman, D. L.; Lynden-Bell, R. M. *Mol. Phys.* **2001**, *99*, 1011.